Optical Properties of Strain-balanced $InAs/InAs_{1-x}Sb_x$ Type-II Superlattices

E. H. Steenbergen[a], Y. Huang[b], J.-H. Ryou[b], R. D. Dupuis[b], K. Nunna[c], D. L. Huffaker[c], and Y.-H. Zhang[a]

[a]*Center for Photonics Innovation and School of Electrical, Computer and Energy Engineering, Arizona State University, Tempe, AZ 85287, USA*
[b]*Center for Compound Semiconductors and School of Electrical and Computer Engineering, Georgia Institute of Technology, Atlanta, GA 30332-0250, USA*
[c]*California NanoSystems Institute, University of California, Los Angeles, CA 90095, USA*

Abstract. Metalorganic chemical vapor deposition- and molecular beam epitaxy-grown strain-balanced $InAs/InAs_{1-x}Sb_x$ type-II superlattices with 20 – 100 periods and Sb composition between $0.22 \leq x \leq 0.30$ exhibit photoluminescence between 5.8 to 10.6 μm at 5 K. The temperature dependent onset of photoresponse obtained from photoconductivity measurements is fit to the Varshni equation, resulting in fitting parameters closer to those of InAs than InSb, and the Fan expression, which gives a Debye temperature less than that of InAs or InSb.

Keywords: superlattice, infrared, photodetector, molecular beam epitaxy, metalorganic chemical vapor deposition.
PACS: 78.67.Pt, 81.15.Hi, 81.15.Gh.

1. INTRODUCTION

InAs/(In)GaSb type-II superlattices (SLs) have been widely studied due to their lower substrate and manufacturing costs, superior uniformity, and higher theoretical quantum efficiency than that of HgCdTe for infrared detector applications. However, the state-of-the-art InAs/(In)GaSb SLs' minority carrier lifetime is still lower than predicted by theory [1]; and complicated interface schemes make them challenging to grow. An alternative type-II SL, $InAs/InAs_{1-x}Sb_x$ SL, is relatively simpler to grow [2, 3] and possibly has less Shockley-Read-Hall recombination [4] due to the absence of Ga. Detailed theoretical modeling work [4] concluded that ideal InAs/(In)GaSb SLs have slightly higher absorption than that of InAs/InAsSb SLs, but the advantages of InAs/InAsSb SLs over the InAs/(In)GaSb SLs are left to experimental demonstration. Recently, strain-balanced $InAs/InAs_{1-x}Sb_x$ multiple-quantum-well structures with Sb composition $x \leq 0.27$ grown by metalorganic chemical vapor deposition (MOCVD) demonstrated photoluminescence (PL) out to 10 μm [5]. This work investigates the optical properties of strain-balanced $InAs/InAs_{1-x}Sb_x$ type-II SLs with $0.22 \leq x \leq 0.30$ grown by MOCVD and molecular beam epitaxy (MBE) on GaSb substrates.

15th International Conference on Narrow Gap Systems (NGS15)
AIP Conf. Proc. 1416, 122-125 (2011); doi: 10.1063/1.3671713

2. RESULTS AND DISCUSSION

InAs/$InAs_{1-x}Sb_x$ SL structures A [100 periods InAs (7.0 nm)/$InAs_{0.76}Sb_{0.22}$ (3.3 nm)] and B [50 periods InAs (7.0 nm)/$InAs_{0.71}Sb_{0.23}$ (2.3 nm)] are grown by MOCVD on 2″ n-GaSb substrates at 500 ℃. Detailed growth conditions are given in reference [3]. Structures C [20 periods InAs (17.6 nm)/$InAs_{0.71}Sb_{0.29}$ (7.0 nm)] and D [60 periods InAs (5.6 nm)/$InAs_{0.70}Sb_{0.30}$ (1.8 nm)] are grown by MBE on 2″ n-GaSb substrates at 435 ℃. The Sb composition in the InAsSb alloy layers is controlled by varying the Sb/As flux ratio. The two growth techniques are interesting to compare as MOCVD offers very high throughput, which is good for mass production, while MBE currently delivers higher quality antimonide materials. The layer thicknesses are chosen to be strain-balanced using the thickness-weighted model, but A and B are found to be 74 % and 83 % relaxed, respectively, according to (224) X-ray diffraction measurements. The designed 0 K effective bandgap energies of structures A, B, C, and D are 224, 250, 105, and 204 meV (5.5, 5.0, 11.8, 6.1 μm), respectively, and are calculated with a 3-band envelope-function approximation model (with the electron, light hole, and spin-orbit bands coupled and the heavy hole decoupled [6]), an InSb/InAs valence band offset of 0.59 eV [7], and 65 % of the InAsSb bandgap bowing occurring in the valence band [8]. The conduction and valence bands of InSb lie higher in energy than those of InAs, leading to a type-II band alignment for InAs and $InAs_{1-x}Sb_x$ [9]. The square of the wave function overlap integral calculated for designs A, B, C, and D are 0.34, 0.31, 0.06, and 0.40, respectively.

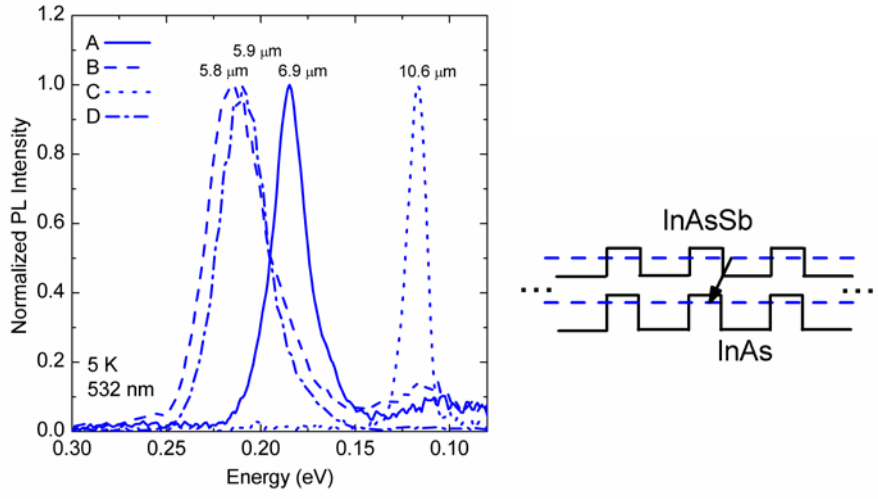

FIGURE 1. a) 5 K photoluminescence spectra for samples A, B, C, and D. b) Schematic of the type-II band alignment between InAs and $InAs_{1-x}Sb_x$.

Figure 1 shows the 5 K PL results obtained using a Fourier transform infrared spectrometer with a 532 nm pump laser at an intensity of 105 W/cm^2 and modulated at 60 kHz (double modulation setup). The discrepancy between the design and the PL peak position is due to the high pump intensity and uncertainties: i) in the material parameters chosen for the model, including the valence band offsets, and ii) in the measurements for x (± 1 %) and the layer thicknesses (± 0.5 nm).

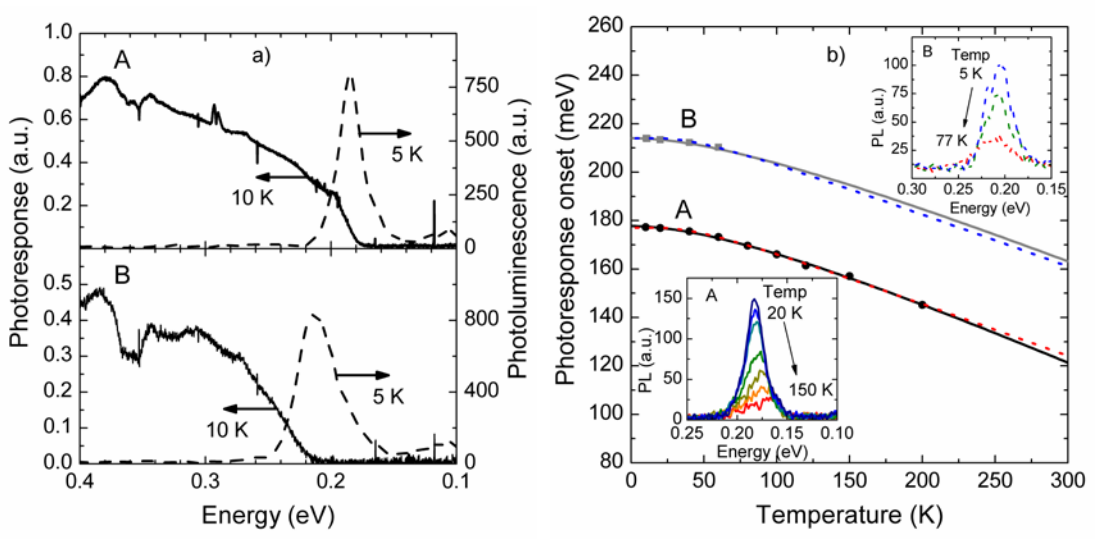

FIGURE 2. a) Photoresponse (photoconductivity) and PL spectra for samples A and B. b) Varshni fit (solid lines) to the absorption onset for samples A and B using $\alpha = 0.275$ meV/K and $\beta = 139$ K and Fan fit (dotted lines) using A = 27.1 meV and $\langle E_p \rangle = 10.7$ meV. Insets: temperature dependent PL.

The spectral photoconductivity is measured with a bias current of 4 mA and 0.5 mA for A and B, respectively, and the signals were corrected for the background using a reference spectrum [10]. Figure 2a shows the PL peak position and the photoresponse onset differ by +8 meV and -1 meV for A and B, respectively. These shifts are mainly due to the band bending, band filling, and bandgap renormalization effects at the present PL pump intensity and the alloy and layer thickness fluctuations in the samples. The broader the PL peak, as is the case for sample B vs. A, the greater the Stokes shift. Sample A gave measurable optical signals up to 200 K, while B only to 77 K. Fitting the photoresponse onset of A to the empirical Varshni equation (see Eq. 1 below) results in fitting parameters $\alpha = 0.275 \pm 0.028$ meV/K and $\beta = 139 \pm 34$ K. α is closer to that of InAs (0.276) than InSb (0.320), but β is between that of InAs (93) and InSb (170) [7]. The InAs layers are thicker than the InAsSb layers, so the parameters are expected to be nearer to the InAs values.

$$E_g(T) = E_g(0) - \frac{\alpha T^2}{(\beta + T)} \tag{1}$$

The analytical Fan expression (see Eq. 2) is also used to fit bandgap temperature dependence [11] and results in the Fan parameter A = 27.1 ± 3.6 meV and the average phonon energy $\langle E_p \rangle = 10.7 \pm 1.1$ meV.

$$E_g(T) = E_g(0) - \frac{A}{\left(e^{\frac{E_p}{kT}} - 1\right)} \tag{2}$$

The Fan parameter for InAs is given as 44 meV and 20 meV and $\langle E_p \rangle$ as 16 meV and 13 meV in [12], which confirm that the SL results are reasonable. The Varshni equation fit (solid lines) and the Fan expression fit (dotted lines) using these same parameters for both A and B are shown in Figure 2b, along with the temperature dependent PL spectra in the insets. The Varshni parameter β is considered to be close to the Debye temperature (Θ_D), which is calculated from the Fan average phonon

energy as $\Theta_D = \langle E_p \rangle / k$. When kT is much greater than $\langle E_p \rangle$, the Varshni and Fan expressions are related by $A/\alpha' = \langle E_p \rangle / k$, where α' is the slope of $E_g(T)$. For T > 100 K, $\alpha' = 0.206$ meV/K, agreeing with the Varshni equation overestimating α [12]. For sample A, $\beta = 139$ K, $\Theta_D = 124$ K, and $A/\alpha' = 131$ K, which are consistent with each other but less than the Debye temperatures for InAs (247 K) and InSb (206 K) [13]. Further temperature dependent analysis on more InAs/InAsSb SL samples is necessary to determine the consistency of the values given here.

3. CONCLUSION

Photoluminescence from 5.8 μm to 10.6 μm for strain-balanced $InAs/InAs_{1-x}Sb_x$ SLs on GaSb with $0.22 \leq x \leq 0.30$ confirm the potential of these SLs to cover wavelengths necessary for mid and long-wavelength infrared applications. The calculated SL effective bandgaps are in reasonable agreement with the experimental results, and the Varshni and Fan expressions are fit to the photoresponse onset temperature dependence.

ACKNOWLEDGMENTS

This work is partially supported by two ARO MURI programs (W911NF-06-1-0353 and W911NF-10-1-0524) and an AFOSR Grant (FA9550-10-1-0129). PL and photoconductance measurements were performed at AFRL/RXPS with the support of G. Brown and B. Ullrich. E.H.S. is supported by the DOD SMART scholarship. Additionally, R.D.D. is thankful for the support of the Steve W. Chaddick Endowed Chair in Electro-Optics and the Georgia Research Alliance.

REFERENCES

1. S. P. Svensson, D. Donetsky, D. Wang, P. Maloney, and G. Belenky, *Proc. SPIE*, **7660**, 76601V (2010).
2. Y.-H. Zhang, *Appl. Phys. Letters* **66**, 118 (1995).
3. Y. Huang, J.-H. Ryou, R. D. Dupuis, V. R. D'Costa, E. H. Steenbergen, J. Fan, Y.-H. Zhang, A. Petschke, M. Mandl, and S.-L. Chuang, *J. Cryst. Growth*, **314**, 92 (2011).
4. C. H. Grein, M. E. Flatte, and H. Ehrenreich, *Proc. 3rd Int. Symp. LWIR Detectors and Arrays: Physics and Applications III*, 211 (1995).
5. D. Lackner, O. J. Pitts, M. Steger, A. Yang, M. L. W. Thewalt, and S. P. Watkins, *Appl. Phys. Lett*ers **95**, 081906 (2009).
6. F. Szmulowicz, E. R. Heller, K. Fisher, and F. L. Madarasz, *Superlattices and Microstructures* **17**, 373-379 (1995).
7. I. Vurgaftman, J. R. Meyer, and L. R. Ram-Mohan, *J. Appl. Physics*, **89**, 5815-5875 (2001).
8. C.-J. Wu, G. Tsai, and H.-H. Lin, *Appl. Phys. Letters* **94**, 211906 (2009).
9. S.-H. Wei and A. Zunger, *Phys. Rev. B* **52**, 12039 (1995).
10. E. H. Steenbergen, Y. Huang, J.-H. Ryou, L. Ouyang, J.-J. Li, D.J. Smith, R.D. Dupuis, and Y.-H. Zhang, *Appl. Phys. Letters* **99**, 071111 (2011).
11. H. Y. Fan, *Phys. Rev*. **82**, 900 (1951).
12. I. A. Vainshtein, A. F. Zatsepin, and V. S. Kortov, *Phys. Solid State* **41**, 907 (1999).
13. H. Warlimont, *Springer handbook of condensed matter and materials data, Vol. 1,* edited by W. Martienssen and H. Warlimont, Berlin Heidelberg: Springer, 2005, pp. 640.